Laboratoire pour l'Utilisation du Rayonnement Electromagnetique at Orsay for the neutron and X-ray facilities.

Registry No. *N,N'*-Methylenebis(acrylamide)·(acrylamide) (copolymer), 25034-58-6; neutron, 12586-31-1.

References and Notes

(1) Weiss, N.; Van Vliet, T.; Silberberg, A. *J. Polym. Sci., Polym. Phys. Ed.* **1979**, *17*, 2229.
(2) Fawcett, J. S.; Morris, C. J. O. R. *Sep. Sci.* **1966**, *1*, 9.
(3) Janas, V. F.; Rodriguez, F.; Cohen, C. *Macromolecules* **1980**, *13*, 977.
(4) Geissler, E.; Hecht, A. M. In "Physical Optics of Dynamical Phenomena and Processes in Macromolecular Systems"; Sedlacek, B., Ed.; de Gruyter: Berlin, 1985; p 157.
(5) Jacrot, B. *Rep. Prog. Phys.* **1976**, *39*, 911.
(6) Hecht, A. M.; Geissler, E. *J. Phys. (Les Ulis, Fr.)* **1978**, *39*, 631.
(7) Geissler, E.; Hecht, A. M.; Duplessix, R. *J. Polym. Sci., Polym. Phys. Ed.* **1982**, *20*, 225.
(8) Daoud, M.; Cotton, J. P.; Farnoux, B.; Jannink, G.; Sarma, G.; Benoit, H.; Duplessix, R.; Picot, C.; de Gennes, P.-G. *Macromolecules* **1975**, *8*, 804.
(9) Dusek, K. In "Polymer Networks"; Chompff, A. J.; Newman, S., Eds.; Plenum Press: New York, 1971; pp 245-260.
(10) Gupta, M. K.; Bansil, R. *J. Polym. Sci., Polym. Lett. Ed.* **1983**, *21*, 969.
(11) Kerker, M. "The Scattering of Light and other Electromagnetic Interactions"; Academic Press: New York, 1969.
(12) Kirste, R. G.; Oberthür, R. C. In "Small Angle X-ray Scattering"; Glatter, O., Kratky, O., Eds.; Academic Press: London, 1982; pp 387-431.
(13) Cotton, J. P.; Nierlich, M.; Boué, F.; Daoud, M.; Farnoux, B.; Jannink, G.; Duplessix, R.; Picot, C. *J. Chem. Phys.* **1976**, *65*, 1101.
(14) Porod, G. In "Small Angle X-ray Scattering"; Glatter, O., Kratky, O., Eds.; Academic Press: London, 1982; pp 17-51.
(15) Kostorz, G. "Small Angle X-ray Scattering"; Glater, O., Kratky, O., Eds.; Academic Press: London, 1982; pp 467-498.
(16) Schaefer, D. W.; Keefer, K. D. *Phys. Rev. Lett.* **1984**, *53*, 1383.
(17) Mandelbrot, B. "The Fractal Geometry of Nature"; W. H. Freeman: San Francisco, 1982.

Polyurethane Interpenetrating Polymer Networks (IPN's) Synthesized under High Pressure. 4. Compositional Variation of Polyurethane–Polystyrene IPN's and Linear Blends

Doo Sung Lee

Department of Textile Engineering, Sung Kyun Kwan University, Suwon, Kyungki 170, Republic of Korea

Sung Chul Kim*

Department of Chemical Engineering, Korea Advanced Institute of Science and Technology, Chongyangni, Seoul 131, Republic of Korea. *Received January 30, 1985*

ABSTRACT: A series of interpenetrating polymer networks and linear blends of polyurethane–polystyrene with different compositions were synthesized under high pressure. The relative order of the degree of mixing of the IPN's was PU75PS25, PU50PS50, and PU25PS75. The dynamic complex modulus behavior followed the theoretical model of Budiansky, which showed phase inversion when the IPN's were synthesized at atmospheric pressure, and followed the Dickie model with glassy matrix when synthesized at 10 000 kg/cm^2 pressure. The morphology via transmission electron microscopy agrees well with the glass transition and modulus behavior. The increased density of IPN's synthesized at high pressure is due to the increase of the degree of mixing and the densification of the polystyrene network. The swelling data indicate that there might be some effect of the interactions caused by the interpenetration of the PU and PS network.

Introduction

Interpenetrating polymer networks (IPN's) can be defined as a mixture of two or more cross-linked polymer networks that have partial or total physical interlocking between them. This subject has been reviewed several times recently.[1-3] The incompatibility of the IPN's arises from the usually low entropy of mixing obtained on blending the high molecular weight polymers, like other polyblend systems. The interpenetration plays a significant role in enhancing the compatibility of the polymer components due to the fact that the physical interlocking prohibits the phase separation from occurring.[4] IPN's exhibit varying degrees of phase separation depending, primarily, on the respective compatibilities of the constituent polymers and, secondly, on the relative rate of network formation and the rate of phase separation.[5] The rate of phase separation is controlled by the mobility of the polymer segment and is related to T_g, molecular weight, and synthesis temperature and pressure.

In the previous papers of this series,[5-7] the synthesis pressure and temperature effects on the miscibility and properties of PU–PMMA IPN's, PU–PS IPN's, semi-IPN's, and linear blends were discussed. The phase separation mechanism when the IPN's were synthesized under high pressure was proposed with relation to the Gibb's free energy of mixing, conversion, the mobility of the polymer segment, and cross-link density. The effect of physical interlocking characteristics was also illustrated. However, the composition of the component polymers was held at 50/50% by weight in the previous papers.

In this paper, the properties of the polyurethane–polystyrene IPN's and linear blends with compositional variations will be discussed.

Experimental Section

Synthesis. The synthesis of the polyurethane–polystyrene IPN's and linear blends was reported elsewhere.[5,7] The PU component was formed by reacting poly(tetramethylene ether) glycol–MDI prepolymer with chain extender (1:1 equivalent ratio of 1,4-butanediol and trimethylolpropane). The cross-linking agent of the PS network was divinylbenzene (55% purity reagent, 2.5 wt % in styrene monomer). The cross-link densities of both networks were set at $\bar{M}_c$ = 3200. The linear blends were formed by excluding the appropriate cross-linking agents in both component polymer formulations. The PU component was reacted at room temperature for 24 h for partial polymerization before the high-pressure reaction. This could be considered to be a kind of SIN with a different polymerization rate. The method of high-pressure synthesis was the same as described before.[5,7] The samples were coded for convenience of presentation. The first

0024-9297/85/2218-2173$01.50/0

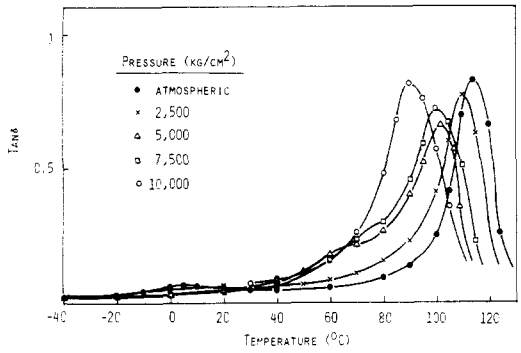

Figure 1. Dissipation factor (tan δ) vs. temperature of UC25SC75 IPN's synthesized at varying pressures.

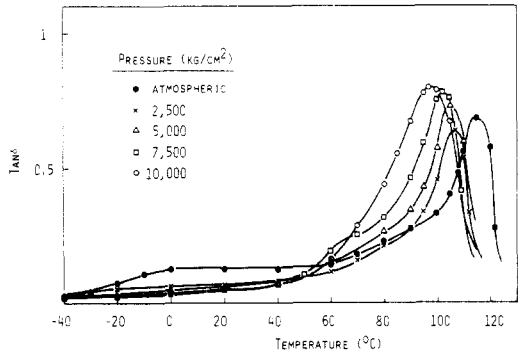

Figure 2. Dissipation factor (tan δ) vs. temperature of UL25SL75 linear blends synthesized at varying pressures.

letter denotes polymer component (U for PU and S for PS), the second letters C and L denote polymer network (C for cross-linked and L for linear), and the third numeral denotes the weight percentage of the polymer.

Measurement. An electron microscope, dynamic mechanical analyzer, and density gradient column were used to observe the morphology, glass transition behavior, and density of the samples prepared. The testing methods were described in the previous paper.[6] A Du Pont Model 951 thermogravimetric analyzer was used to measure the thermal stability. The sample weight was about 10 mg, N_2 flow rate was 120 cm^3/min, and the heating rate was 20 °C/min.

Results and Discussion

Dynamic Mechanical Behavior. The dynamic mechanical behavior of the PU–PS IPN's and the linear blends with different compositions synthesized under varying pressures is shown in Figures 1–4. Figures 1 and 2 show the tan δ change of PU25PS75 IPN and linear blend. There is a gradual shift of the transition temperature of the PS component as the pressure is increased. The PS phase damping is very high, while the PU phase transition is not shown distinctly due to the low concentration of PU component. The tan δ curves for the PU75PS25 IPN and linear blend (Figure 3 and 4) show the gradual inward shift of the PU transition. The PS phase transition could not be detected due to the instrumental limitation of the Du Pont 981 DMA. These curves also show the inward shift and the broadening of the PU transition as the pressure is increased. The UL75SL25 linear blends synthesized above atmospheric pressure show a broader transition than the UC75SC25 IPN's because of a higher degree of phase separation due to the absence of physical interlocking.

The T_g of the PS-dominant phase (PU25PS75) and of the PU-dominant phase (PU75PS25) is shown in Table I. The T_g of UL75SL25 could not be measured because of the very broad transition characteristics. The mass fractions in the PS-dominant phase of PU25PS75 and the

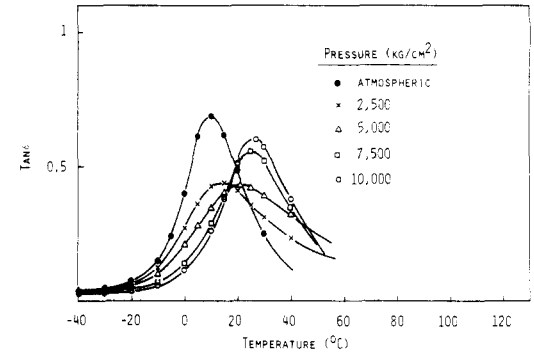

Figure 3. Dissipation factor (tan δ) vs. temperature of UC75SC25 IPN's synthesized at varying pressures.

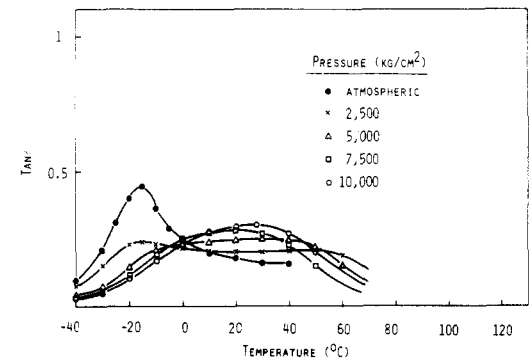

Figure 4. Dissipation factor (tan δ) vs. temperature of UL75SL25 linear blends synthesized at varying pressures.

Table I
T_g and Composition in the PS-Dominant Phase (for PU25PS75 IPN and Linear Blend) and in the PU-Dominant Phase (for UC75SC25 IPN)

sample code	synth press, kg/cm²	T_g, K	compn PU	compn PS
UC25SC75	atm	387	0.02	0.98
	2500	383	0.05	0.95
	5000	375	0.10	0.90
	7500	373	0.11	0.89
	10000	363	0.19	0.81
UL25SL75	atm	388	0	1.00
	2500	380	0.04	0.96
	5000	378	0.05	0.95
	7500	375	0.06	0.94
	10000	370	0.09	0.91
UC75SC25	atm	283	0.94	0.06
	2500	288	0.88	0.12
	5000	294	0.81	0.19
	7500	298	0.77	0.23
	10000	300	0.75	0.25

PU-dominant phase of PU75PS25 calculated by assuming the Fox equation are shown in Table I and Figure 5. The PU mass fraction in the PS-dominant phase of the PU25PS75 increases as the synthesis pressure is increased. The PU mass fraction in the PU-dominant phase of PU75PS25 decreases as the intermixing increases with increasing pressure. The UL25SL75 linear blend shows a lower degree of mixing than the UC25SC75 IPN due to the absence of physical interlocking and the high mobility of the linear PU chain.

To compare the degree of intermixing as the compositions change, the relative degree of mixing is expressed as the ratio of the mass fraction in the PS- or PU-dominant phase calculated by the Fox equation (from the T_g shift) and the maximum mass fraction in the completely mixed state. The degree of mixing of the UC75SC25 IPN is slightly higher than that of the UC50SC50 IPN, and these

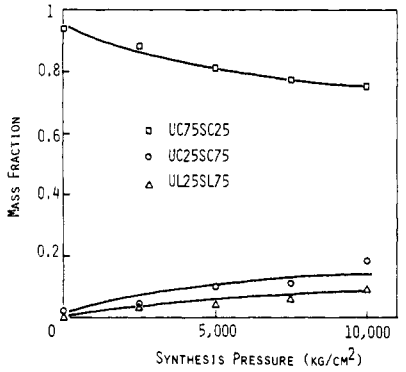

Figure 5. Calculated mass fraction of PU in the PS-dominant phase of UC25SC75 and UL25SL75 and in the PU-dominant phase of UC75SC25 IPN.

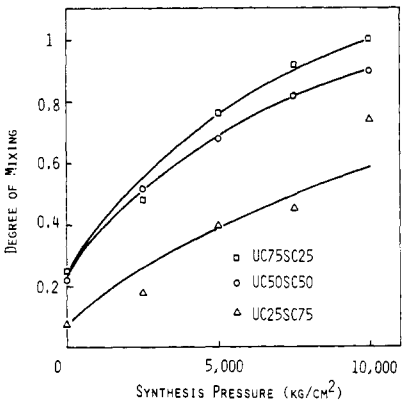

Figure 6. Calculated degree of mixing vs. synthesis pressure of the IPN's.

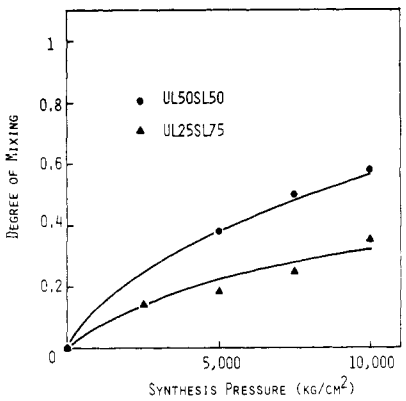

Figure 7. Calculated degree of mixing vs. synthesis pressure of the linear blends.

two IPN's show a much higher degree of mixing than the UC25SC75 IPN (Figure 6). The UL50SL50 linear blend also has a higher degree of mixing than the UL25SL75 linear blend (Figure 7). Since most polymer–polymer systems generally exhibit LCST (lower critical solution temperature) behavior,[8-10] a schematic phase diagram like the one in Figure 8 can be proposed from the above results. The LCST is considered to shift to a higher temperature with increasing synthesis pressure.

The dynamic Young's modulus vs. temperature plots of the PU–PS IPN's with compositions of 25/75, 50/50, and 75/25% synthesized at atmospheric pressure and 10 000 kg/cm^2 are shown in Figure 9. The IPN's synthesized at 10 000 kg/cm^2 show one sharp transition, which implies a homogeneous single-phase polymer blend, while the IPN's synthesized at atmospheric pressure show two separated transitions of modulus, which mean the heterogeneous two-phase polymer blend. These results are in agreement with the tan δ vs. temperature plot.

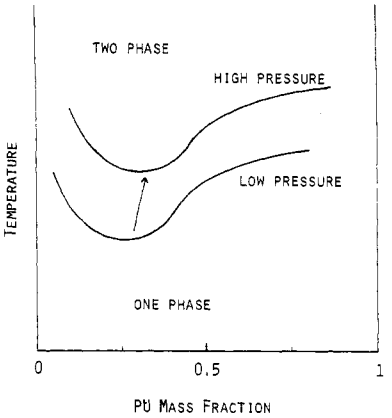

Figure 8. Schematic of the phase diagram of the PU–PS polymer composite showing LCST behavior.

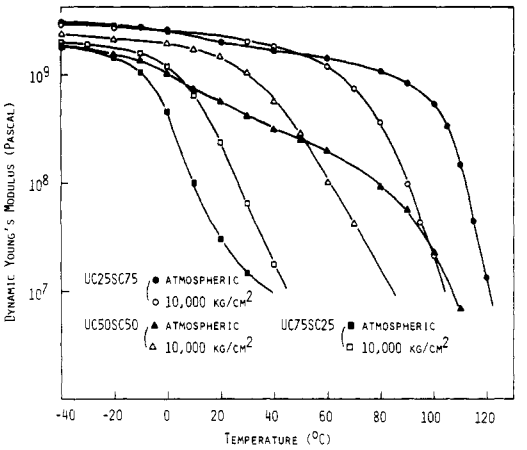

Figure 9. Dynamic Young's modulus vs. temperature of the IPN's synthesized at atmospheric pressure and 10 000 kg/cm^2.

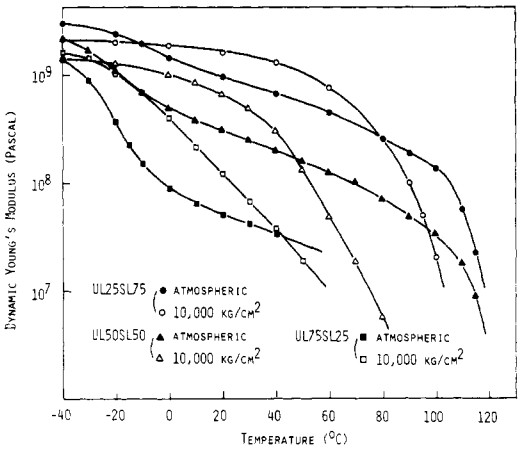

Figure 10. Dynamic Young's modulus vs. temperature of the linear blends synthesized at atmospheric pressure and 10 000 kg/cm^2.

Similar behavior is also observed in the dynamic Young's modulus vs. temperature plot of the linear blends (Figure 10). At the atmospheric synthesis pressure, the UL75SL25 linear blend shows a higher modulus above room temperature than the UC75SC25 IPN, which seems to be due to the crystallization of the linear polyurethane.[11]

Composition Models. The modulus–composition behavior of the PU–PS IPN's and linear blends was analyzed with some of the theoretical equations based on mechanical models. Most of these models assumed perfect adhesion

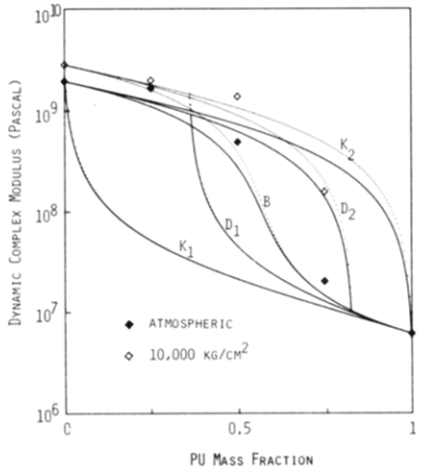

Figure 11. Dynamic complex Young's modulus at 23 °C vs. PU concentration for the PU–PS IPN's synthesized at atmospheric pressure and 10000 kg/cm^2. Solid lines and dotted lines are based on the theoretical models for the atmospheric pressure and 10000 kg/cm^2, respectively, with K_1, the Kerner model, assuming the PU phase as the continuous phase, K_2 assuming the PS phase as the continuous phase, D_1 and D_2 as the respective Dickie models, and B as the Budiansky model.

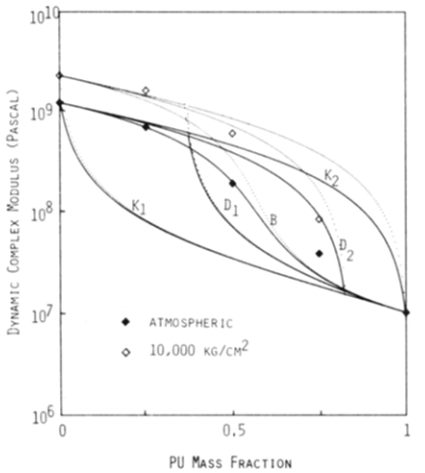

Figure 12. Dynamic complex Young's modulus at 23 °C vs. PU concentration for the PU–PS linear blends synthesized at atmospheric pressure and 10000 kg/cm^2. All notations are same as those of Figure 11.

between the matrix and the spherical inclusion (dispersion). They were discussed and reviewed by Nielsen[12] and Dickie.[13-15]

The Kerner equation,[16] the Dickie equation,[14] and the Budiansky equation[17] were compared with the experimental dynamic complex Young's modulus results at 23 °C (Figures 11 and 12). The theoretical models for the polymer composites synthesized at atmospheric pressure (solid line) and 10000 kg/cm^2 (dotted line) are plotted in the figure with the experimental data.

The complex Young's modulus–composition data at 23 °C of IPN's and linear blends synthesized at atmospheric pressure show a better fit with the Budiansky model (denoted as B in the figure) than with the other models. The theoretically predicted modulus values for high PU concentration with the elastomeric matrix (B, K_1, and D_1 in the figure) and for high PS concentration with the rigid matrix (B, K_2, and D_2 in the figure) show little difference between the models. The predicted values differ widely at intermediate PU concentration, and the better fit with the Budiansky model is quite expected since the assumptions made in deriving the equation represent the phase-inversion process well. Similar results were reported by

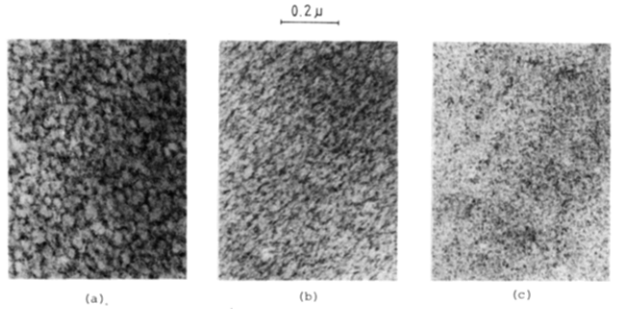

Figure 13. Electron micrographs of UC25SC75 IPN's synthesized at (a) atmospheric pressure, (b) 5000 kg/cm^2, and (c) 10000 kg/cm^2.

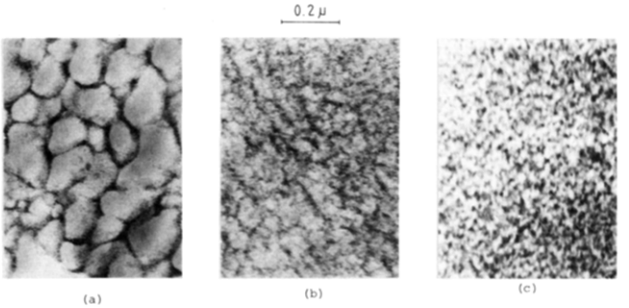

Figure 14. Electron micrographs of UL25SL75 linear blends synthesized at (a) atmospheric pressure, (b) 5000 kg/cm^2, and (c) 10000 kg/cm^2.

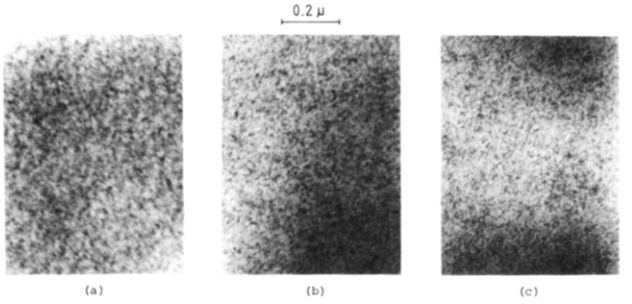

Figure 15. Electron micrographs of UC75SC25 IPN's synthesized at (a) atmospheric pressure, (b) 5000 kg/cm^2, and (c) 10000 kg/cm^2.

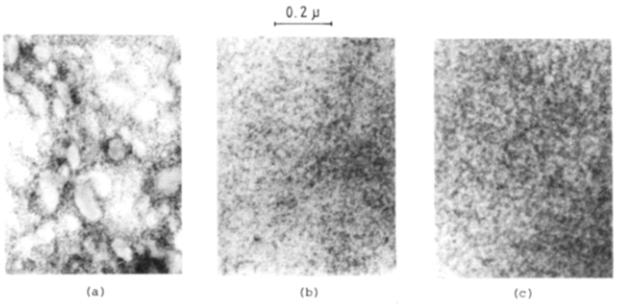

Figure 16. Electron micrographs of UL75SL25 synthesized at (a) atmospheric pressure, (b) 5000 kg/cm^2, and (c) 10000 kg/cm^2.

Kim et al.[11] and Frisch et al.[18] for the polyurethane–poly(methyl methacrylate) IPN and the polyurethane–acrylic copolymer IPN.

The modulus–composition data at 23 °C of the IPN's and linear blends synthesized at 10000 kg/cm^2 show a better fit with the Dickie model with the rigid matrix which is based on a polymer composite where the matrix and the dispersed phase are well defined. This result agrees well with the morphology results described in this paper and the previous papers,[5,7] which showed a completely dispersed PU domain when synthesized at high pressure.

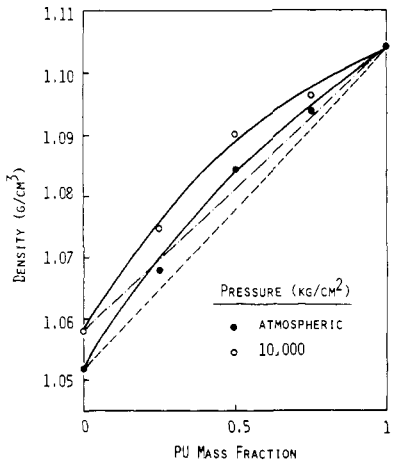

Figure 17. Density vs. PU composition of the IPN's synthesized at atmospheric pressure and 10 000 kg/cm^2. Straight lines are based on volume additivity rule.

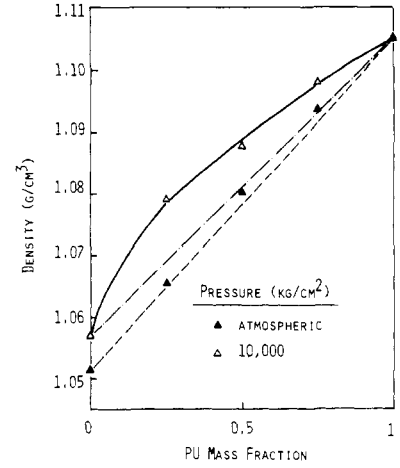

Figure 18. Density vs. PU composition of the linear blends synthesized at atmospheric pressure and 10 000 kg/cm^2. Straight lines are based on volume additivity rule.

Morphology. The morphology via transmission electron microscopy also shows the synthesis pressure effects on the polymer miscibility and phase structure. It agrees well with the miscibility behavior observed by the dynamic mechanical properties (Figures 13–16).

The UC25SC75 IPN synthesized at atmospheric pressure (Figure 13a) shows a dispersed PS phase with a domain size of about 500 Å. A secondary phase separation at the PU-rich phase that forms an apparent continuous phase (as described in the previous paper) is also shown. At the synthesis pressure of 5000 kg/cm^2, the phase structure becomes somewhat cocontiuous in the decreased domain size of the PS-dominant phase (Figure 13b). The fine dispersed PU with domain size of about 100 Å is shown in the case of 10 000 kg/cm^2 (Figure 13c).

For the UL25SL75 linear blend synthesized at atmospheric pressure (Figure 14a), the large distinct PS domains with sizes of about 2000 Å are shown. As the synthesis pressure is increased, a similar domain structure as the UC25SC75 IPN is developed, but the domain size is larger than that of UC25SC75.

The UC75SC25 IPN's show that the PU phase is continuous when synthesized at atmospheric pressure, but the PS phase becomes continuous when synthesized at 10 000 kg/cm^2 with the very fine dispersed PU phase (Figure 15). A complex phase structure with the PS-dispersed domain of about 1000 Å appears when the UL75SL25 linear blend is synthesized at atmospheric pressure, but again the PS phase becomes continuous when synthesized at 10 000 kg/cm^2 (Figure 16).

The synthesis method of IPN was a kind of simultaneous polymerization method with a different reaction rate. It is very interesting to note that the PU phase is continuous even for the high PS concentration in UC25SC75 IPN (Figure 13a) when the synthesis pressure is atmospheric, mainly due to the fact that the PU phase is formed earlier, but the PS phase always becomes a continuous matrix even for the IPN's with high PU concentration (UC75SC25 IPN, Figure 15c) when the synthesis pressure is 10 000 kg/cm^2.

Density. The density vs. PU composition of the IPN's and linear blends synthesized at atmospheric pressure and 10 000 kg/cm^2 is shown in Figures 17 and 18.

The IPN's synthesized at both atmospheric pressure and 10 000 kg/cm^2 show increased densities over the calculated densities based on the volume additivity of the components, and this increase seems to be due to the increase of the degree of mixing. Although the synthesis pressure is increased to 10 000 kg/cm^2 and the degree of mixing increased as well, the density difference between the experimental and calculated values is nearly constant in IPN's synthesized at both atmospheric pressure and 10 000 kg/cm^2. The high density values in the IPN's synthesized at high pressure are mainly due to the densification in the PS network. The fact that there is no significant increase in density above 2500 kg/cm^2 as described in the previous papers[5,7] is due to the limitation of PS densification.

In the case of linear blends, when the synthesis pressure is atmospheric, the densities are similar to calculated values based on volume additivity because the degree of mixing is near zero, but when the synthesis pressure is 10 000 kg/cm^2, the increased densities were due to the increased degree of mixing and the densification by pressure.

Swelling Behavior. The Flory–Rehner[19] equilibrium swelling equation has long been used to characterize single-component polymer-network properties. Recently, Thiele and Cohen[20] derived a corresponding equation for homo-IPN's, in which networks I and II are identical in chemical composition but have different cross-link densities.

$$\ln (1 - v_1 - v_2) + v_1 + v_2 + \chi_s(v_1 + v_2)^2 = -V_s N_1'(v_1^{1/3} - 2v_1/F_1) - V_s N_2'(v_2^{\circ 2/3} v_2^{1/3} - 2v_2/F_2) \quad (1)$$

Siegfried et al.[21] modified the Thiele–Cohen equation through the addition of a thermoplastic front factor to account for the internal energy changes due to swelling.[21-23] The modified equation reads

$$\ln (1 - v_1 - v_2) + v_1 + v_2 + \chi_s(v_1 + v_2)^2 = -V_s N_1'(1/v_1^\circ)^{2/3}(v_1^{1/3} - 2v_1/F_1) - V_s N_2'(v_2^{\circ 2/3} v_2^{1/3} - 2v_2/F_2) \quad (2)$$

where v_1 and v_2 are the volume fractions of polymers I and II in the swollen state, v_1° and v_2° are the volume fractions of polymers I and II in the unswollen state, V_s is the molar volume of the solvent, N_1' and N_2' are the cross-link densities of the homopolymer networks (in mol/cm^3), χ_s is the polymer–solvent interaction parameter, and F_1 and F_2 are the functionalities of the systems.[24] In the derivation of both the unmodified and modified Thiele–Cohen equation, χ_s was assumed to be identical for both polymers. For the present case, a simple average of the two values was assumed for χ_s[25]

$$\bar{\chi}_s = w_1\chi_1 + w_2\chi_2 \quad (3)$$

where $\bar{\chi}_s$ is the average interaction parameter for the IPN, w_1 and w_2 are the weight fractions of polymers I and II, and χ_1 and χ_2 are the interaction parameters for homopolymers I and II, respectively.

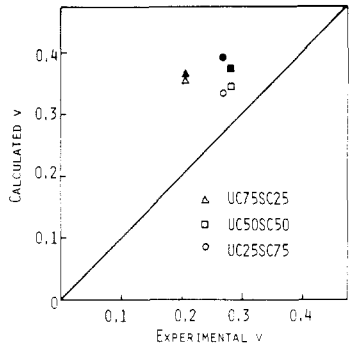

Figure 19. Experimental value v vs. v as predicted by the unmodified (open symbol) and modified (closed symbol) Thiele–Cohen equation for the IPN's synthesized at atmospheric pressure.

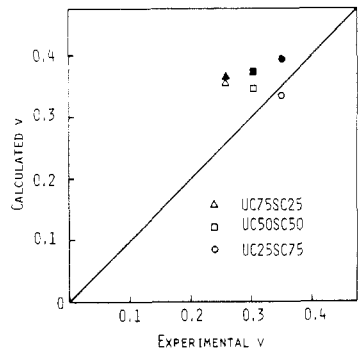

Figure 20. Experimental value v vs. v as predicted by the unmodified (open symbol) and modified (closed symbol) Thiele–Cohen equation for the IPN's synthesized at 10 000 kg/cm^2.

The swelling behavior of IPN's and homopolymers was examined by equilibrium swelling in 1,4-dioxane. The theoretical network chain concentrations N of the homopolyurethane and homopolystyrene networks were calculated to be 1.75×10^{-4} and 2.22×10^{-4} mol/cm^3 from the stoichiometry. With the assumption that the theoretical and experimental network chain concentrations are equal and by the use of the experimental volume fractions of homopolymer in the swollen state (PU, 0.371; PS, 0.274), the unknown polymer–solvent interaction parameters could be estimated from the Flory–Rehner equation. The estimated χ_1 (for PU) and χ_2 (for PS) were 0.62 and 0.49, respectively. Siegfried et al.[21] have shown that the theoretical and experimental N of the homopolymer PS networks agree fairly well.

By the use of theoretical N, the experimental v_1 and v_2, and the calculated χ_1 and χ_2, the calculated volume fractions of IPN's in the swollen state, v (or $v_1 + v_2$), were estimated from eq 1 and 2.

Values for v obtained from eq 1 and 2 vs. v's determined from the swelling experiment are shown in Figure 19 (IPN's made at atmospheric pressure) and Figure 20 (IPN's made at 10 000 kg/cm^2). If there exists additional physical and chemical cross-linking during IPN formation, the data are expected to shift to the right of the diagonal line. Figures 19 and 20 indicate that no new pysical or chemical cross-links are present and that the experimental degree of swelling is greater than the predicted value.[25,26]

The volume fractions of polymer in the swollen state vs. PU mass fraction for the IPN's formed at atmospheric pressure and 10 000 kg/cm^2 are shown in Figure 21. The degree of swelling of homo-PS is much higher than that of homo-PU prepared at atmospheric pressure and 10 000 kg/cm^2. The degree of swelling of the IPN's synthesized at atmospheric pressure is higher than that of the IPN's synthesized at 10 000 kg/cm^2 over the entire range of PU composition. The morphological change, e.g., the phase

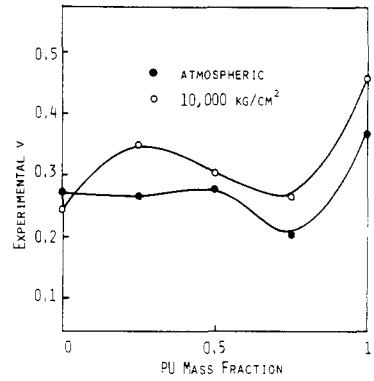

Figure 21. Experimental value v vs. PU mass fraction for the IPN's synthesized at atmospheric pressure and 10 000 kg/cm^2.

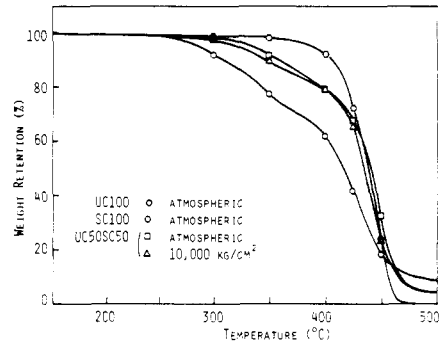

Figure 22. TGA thermograms for PU–PS IPN's.

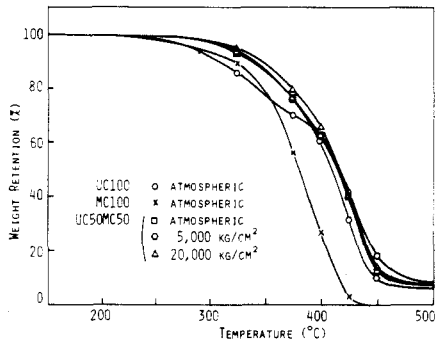

Figure 23. TGA thermograms for PU–PMMA IPN's.

domain size and phase continuity and the cross-link density increase during the high-pressure synthesis (refer to Figures 19 and 20), should be considered in explaining the above swelling behavior. It is interesting that UC25SC75 IPN's prepared at 10 000 kg/cm^2 show maximum v (refer to Figure 21) and UC75SC25 IPN's prepared at both atmospheric pressure and 10 000 kg/cm^2 show minimum v. The maximum is observed at low PU concentration and the minimum is observed at high PU concentration range. This behavior cannot be explained by the morphological change alone. We think it might be related to the interactions caused by the interpenetration of the PU and PS networks. The presence of a PS chain penetrated inside the PU domain could reduce the hydrogen bonding of the PU network and might increase swelling (low v).

Thermal Stability. The enhancement of the thermal stability of PU–PMMA and PU–PS IPN's was reported, and it was presumed that the unzipped MMA or styrene monomer acted as the radical scavenger for the radicals produced from the PU degradation.[27] The PU–PMMA and PU–PS IPN's synthesized at atmospheric pressure, which was prepared in this series, also showed enhancement of weight retention compared to the proportional average of the weight retentions of the pure components.

But the additional enhancement of the thermal stability expected due to the increased miscibility in IPN's synthesized under high pressure was not observed (Figures 22 and 23). In other words, the weight loss was independent of synthesis pressure.

Acknowledgment. This work was supported by the Korea Science and Engineering Foundation. We thank Dr. J. K. Yeo and C. M. Oh of Lucky Ltd. for their help in the electron microscopy work.

Registry No. (1,4-Butanediol)·(polytetramethylene glycol)·(trimethylolpropane)·(MDI) (copolymer), 39281-41-9; (divinylbenzene)·(styrene) (copolymer), 9003-70-7; (1,4-butanediol)·(MDI)·(polytetramethylene glycol) (copolymer), 9018-04-6; polystyrene (homopolymer), 9003-53-6.

References and Notes

(1) Manson, J. A.; Sperling, L. H. "Polymer Blends and Composites"; Plenum Press: New York, 1976.
(2) Sperling, L. H. "Interpenetrating Polymer Networks and Related Materials"; Plenum Press: New York, 1981.
(3) Klempner, D.; Frisch, K. C. "Polymer Alloys"; Plenum Press: New York, 1977.
(4) Kim, S. C.; Klempner, D.; Frisch, K. C.; Radigan, W.; Frisch, H. L. *Macromolecules* **1976**, *9*, 258.
(5) Lee, D. S.; Kim, S. C. *Macromolecules* **1984**, *17*, 2193.
(6) Lee, D. S.; Kim, S. C. *Macromolecules* **1984**, 17, 268.
(7) Lee, D. S.; Kim, S. C. *Macromolecules* **1984**, *17*, 2222.
(8) Bernstein, R. E.; Cruz, C. A.; Paul, D. R.; Barlow, J. W. *Macromolecules* **1977**, *10*, 681.
(9) Robard, A.; Patterson, D. *Macromolecules* **1977**, *10*, 1021.
(10) Patterson, D.; Robard, A. *Macromolecules* **1978**, *11*, 690.
(11) Kim, S. C.; Klempner, D.; Frisch, K. C.; Frisch, H. L. *Macromolecules* **1977**, *10*, 1187 and 1191.
(12) Nielsen, L. E. "Mechanical Properties of Polymers and Composites"; Marcel Dekker: New York, 1974; Vol. 2, 395.
(13) Dickie, R. A. *J. Appl. Polym. Sci.* **1973**, *17*, 45 and 2509.
(14) Dickie, R. A.; Cheung, M. F.; Newman, S. *J. Appl. Polym. Sci.* **1973**, *17*, 65.
(15) Dickie, R. A.; Cheung, M. F. *J. Appl. Polym. Sci.* **1973**, *17*, 79.
(16) Kerner, E. H. *Proc. Phys. Soc., London, Sect. B.* **1956**, *69*, 808.
(17) Budiansky, B. *J. Mech. Phys. Solids* **1965**, *13*, 223.
(18) Frisch, K. C.; Klempner, D.; Frisch, H. L. *Polym. Eng. Sci.* **1982**, *22*, 1143.
(19) Flory, P. J.; Rehner, J. *J. Chem. Phys.* **1943**, *11*, 512.
(20) Thiele, J. L.; Cohen, R. E. *Polym. Eng. Sci.* **1979**, *19*, 284.
(21) Siegfried, D. L.; Thomas, D. A.; Sperling, L. H. *Macromolecules* **1979**, *12*, 586.
(22) Tobolsky, A. V.; Shen, M. C. *J. Appl. Phys.* **1966**, *37*, 1952.
(23) Galanti, A. V.; Sperling, L. H. *Polym. Eng. Sci.* **1970**, *10*, 177.
(24) Bell, J. P. *J. Polym. Sci., Part A-2* **1970**, *6*, 417.
(25) Hargest, S. C.; Manson, J. A.; Sperling, L. H. *J. Appl. Polym. Sci.* **1980**, *25*, 469.
(26) Lipatov, Y. S.; Sergeeva, L. M.; Mozzhukhina, L. V.; Apukhtina, N. P. *Polym. Sci. USSR (Engl. Transl.)* **1974**, *16*, 2658.
(27) Kim, S. C.; Klempner, D.; Frisch, K. C.; Frisch, H. L. *J. Appl. Polym. Sci.* **1977**, *21*, 1289.

Study of Miscibility and Critical Phenomena of Deuterated Polystyrene and Hydrogenated Poly(vinyl methyl ether) by Small-Angle Neutron Scattering

Mitsuhiro Shibayama,† Hsinjin Yang, and Richard S. Stein*

Polymer Research Institute, University of Massachusetts, Amherst, Massachusetts 01003

Charles C. Han

National Bureau of Standards, Gaithersburg, Maryland 20899. *Received December 7, 1984*

ABSTRACT: Miscibility and critical phenomena were studied on the polymer system of deuterated polystyrene and hydrogenated poly(vinyl methyl ether) by the small-angle neutron scattering technique. The phase diagram was constructed with "light" and "neutron" cloud points as well as spinodal points. It shows a well-known behavior of a lower critical solution temperature. The agreement between the "light" and "neutron" cloud points is fairly good for all compositions. The correlation length, the statistical segment length, and the Flory–Huggins χ-parameter were obtained as functions of temperature and composition by employing de Gennes' scattering equation for polymer blends. The χ-parameter showed not only a temperature dependence but also a composition dependence. Comparison of the χ-parameter with the lattice fluid theory shows that the composition dependence of χ results from the lattice fluid nature of the system, i.e., the compressibility and the thermal expansion of the system.

I. Introduction

After the discovery of miscible polymer blends,[1] their study has been of great interest. The miscibility has usually been discussed in terms of the Flory–Huggins interaction parameter χ or the second virial coefficient A_2. In these studies, small-angle neutron scattering (SANS) is one of the most powerful methods for obtaining the χ-parameter because of the high contrast between labeled and unlabeled species. Zimm analyses have usually been done making the analogy of polymer–solvent systems,[2] which is only valid for dilute systems. Recently, the theory has been extended to apply to concentrated polymer–polymer mixtures,[3-7] where the concentration dependence of the χ-parameter became apparent.[8,9] Prior to SANS experiments, the concentration dependence of the χ-parameter had been observed by 1950.[10] Koningsveld et al. used this concentration dependence to explain their light scattering experiment results in polymer–solvent systems[11] and later polymer–polymer systems.[12] Although the existence of the lower critical solution temperature (LCST) was explained by introducing the equation of state theory[13,14] and the lattice fluid theory,[15,16] the concentration dependence of the χ-parameter has not been well understood. The correlation length is also a measure of the miscibility and plays an important role in the vicinity of the critical point.

We have reported a novel method for obtaining the cloud point in a polymer blend by SANS,[17] the "neutron"

† Present address: Department of Polymer Science and Engineering, Faculty of Textile Science, Kyoto Institute of Technology, Matsugasaki, Sakyo-ku, Kyoto, 606 Japan.

0024-9297/85/2218-2179$01.50/0